공학석사학위논문

난류 평판 유동에서 화학반응 파울링에 대한 직접수치모사

Direct numerical simulation of chemical reaction fouling in a turbulent channel flow

2017 년 2 월

서울대학교 대학원

기계항공공학부

김 한 별

Direct numerical simulation of chemical reaction fouling in a turbulent channel flow

Hanbyeol Kim

Department of Mechanical & Aerospace Engineering
Seoul National University

Abstract

In heat exchanger industries, the fouling deposition on solid surfaces causes serious problems such as impaired heat transfer and increased pressure drop. Thus, the prediction and mitigation of fouling deposits has been an important issue. In the present study, we conduct direct numerical simulation of a fully developed channel flow. We assume that fluid flows as a slurry flow and the apparent viscosity is calculated using Thomas' equation. We also assume that a second order reaction with single soluble reactant occurs and a highly viscous product is accumulated at high-temperature wall. Two passive scalar equations are solved along with the Navier-Stokes equations to obtain the mass fraction of the reactant and the temperature in the channel. The reactant flows into the channel at the inlet, and the highly viscous product is stuck on the wall and forms a fouling layer.

Keyword : CFD, numerical modeling, chemical reaction fouling, asphaltene, channel flow

Student Number : 2012-23939

Contents

List of Figures

Nomenclature

Roman symbols

p	Pressure
C	Volume fraction of coke
Re	Reynolds number, $\mathrm{Re}_{asp}=u_b(2\delta)/\nu_{asp}$
Pr	Prandtl number, $\mathrm{Pr}=\nu/\alpha$
Sc	Schmidt number, $\mathrm{Sc}=\nu/D$
t	Time
x_i	Cartesian coordinates
u_i	Velocity components
u_b	Mean velocity of the channel inlet
D	Mass diffusivity
R_f	Fouling resistance, m^2K/W

Greek symbols

δ	Channel half-height
ν	Kinematic viscosity
μ_r	Relative viscosity
α	Thermal diffusivity
ω_x	Instantaneous streamwise vorticity
ω_z	Instantaneous spanwise vorticity

Subscripts

asp	Asphaltene

Chapter 1

Introduction

Fouling is the accumulation of unwanted material on solid surfaces to the detriment of function. The fouling material consists of either living organisms (bio-fouling) or non-living substance. In crude oil and electric-device industries, the chemical reaction fouling on solid surfaces causes serious problems such as the deterioration of heat transfer and the pressure drop. Thus, the prediction and mitigation of the fouling deposits is an important subject to investigate. The estimated losses due to fouling of heat exchanger in industrialized nations are about 0.25% of their GDP (Müller-Steinhagen *et al.*, 2005). The economic loss owing to boiler and turbine in China utilities is about 4.68 billion dollars, which is 0.169% of the country GDP (Zhi-Ming *et al.*, 2007).

There are some experimental studies about chemical reaction fouling. Helaizadeh *et al.* conducted experiments on mixed salt crystallization fouling (Helaizadeh *et al.*, 2000). Also, Mwaba *et al.* investigated crystallization fouling on a heated copper (Mwaba *et al.*, 2006). However, only a few CFD researches on chemical reaction fouling have been done until now. FIGURE 1.1 shows the fouling matrix which divides fouling with its mechanisms and sub-processes. Black areas of the matrix mean that many researches were conducted and white and grey areas mean that little researches have been conducted. Especially, the process of chemical reaction fouling is not fully investigated yet.

For computational investigation of chemical reaction fouling,

Brahim *et al.* conducted two-dimensional flow using k-ε model and empirical correlation (Brahim *et al.*, 2003). Also, asphaltene deposition in crude oil distillation units was investigated using a mathematical model (Sileri *et al.*, 2009). They used a diffuse interface method for interface tracking at low Reynolds number. Bayat *et al.* simulated fouling of crude oil in a two-dimensional channel and assumed fouling as a highly viscous fluid (Bayat *et al.*, 2012). Yet previous researches have a limitation of not considering the entire process of chemical reaction fouling. Also, previous studies did not show the interaction between the process of chemical reaction fouling and turbulent flow.

Thus, the aim of the present study is to conduct direct numerical simulation (DNS) of a turbulent channel flow with a chemical reaction based on heat transfer. Furthermore, we are going to investigate the interaction between the chemical reaction fouling and turbulent flow with the attachment and growth of fouling material.

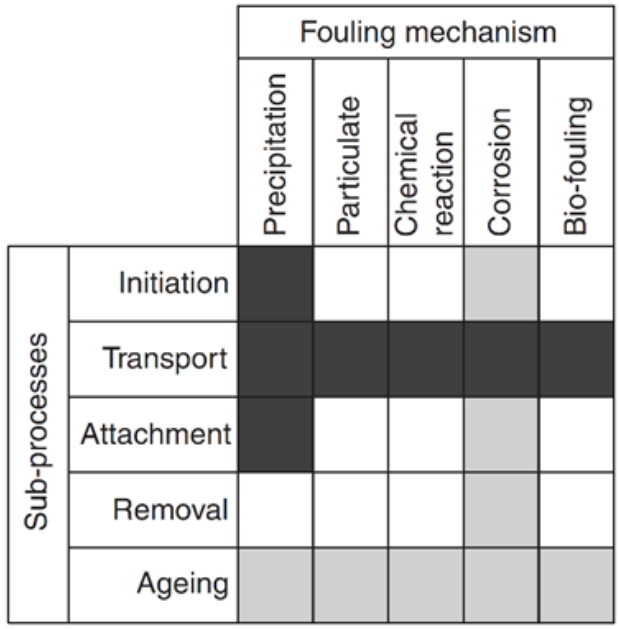

FIGURE 1.1 The 5x5 fouling matrix (Macchietto *et al.*, 2011)

Chapter 2

Numerical Methodology

2.1 Problem description

FIGURE 2.1 shows the schematic diagram of the process of fouling deposition. We assumed that a chemical reaction occurs between two materials, asphaltene and coke. Coke is considered as a highly viscous fluid and we assumed that the entire fluid flows like slurry (Bayat *et al.*, 2012).

As asphaltene flows into the channel, the reaction occurs and the volume fraction of coke increases. As a result, the highly viscous product is stuck near the wall and the apparent viscosity increases near the wall as time goes by. After all, asphaltene can't pass through the fouling region and flows upper the fouling surface. Ultimately the interface of fouling rises from the wall of the channel.

2.2 Governing equations

The governing equations for an incompressible flow are

$$\frac{\partial u_i}{\partial x_i} = 0, \tag{1}$$

$$\frac{\partial u_i}{\partial t} + \frac{\partial u_i u_j}{\partial x_j} = -\frac{\partial p}{\partial x_i} + \frac{1}{Re_{asp}} \frac{\partial}{\partial x_j} \left[\mu_r(C) \left(\frac{\partial u_i}{\partial x_j} + \frac{\partial u_j}{\partial x_i} \right) \right], \tag{2}$$

where x_i' s are the Cartesian coordinates, and u_i' s are the corresponding velocity components. C is the volume fraction of coke, and Re_{asp} is the Reynolds number corresponding to the viscosity of asphaltene. The relative viscosity term in the Navier–Stokes equations plays an important role in the accumulation of fouling. The definition of relative viscosity in the present study is

$$\mu_r = \mu_{entire\ flow} / \mu_{asp}.$$

FIGURE 2.2 shows a plot of volume fraction of solid versus relative viscosity with different equations. Among the existing equations, we chose Thomas' equation which can describe the high viscosity of coke better than other equations. The Thomas' equation is below.

$$\mu_r(C) = 1 + 2.5C + 10.05C^2 + \alpha \cdot e^{\beta C},$$

where α = 0.00273 and β = 16.6. According to the Thomas' equation, the relative viscosity steeply rises as the volume fraction of solid increases.

The Governing equations of the volume fraction and temperature are

$$\frac{\partial C}{\partial t} + \frac{\partial}{\partial x_j}\left(Cu_j\right) = \frac{1}{\mathrm{Re}_{asp}\mathrm{Sc}} \frac{\partial^2 C_R}{\partial x_j \partial x_j} + S(T, C), \tag{3}$$

$$\frac{\partial T}{\partial t} + \frac{\partial}{\partial x_j}\left(Tu_j\right) = \frac{1}{\mathrm{Re}_{asp}\mathrm{Pr}} \frac{\partial^2 T}{\partial x_j \partial x_j}, \tag{4}$$

where T is the temperature of fluid.

$S(T,C)$, which means reaction rate, is obtained from Akmaz *et al.*,

2013 and the specific equation of the reaction rate is below.

$$S(T,C) = k(T)\cdot(1-C)^2,$$
$$k(T) = 0.6905\cdot T^2 + 1.6596\cdot T + 0.9691,$$

where $k(T)$ means the rate constant of reaction which also obtained from Akmaz *et al.* The range of temperature is from 300° C to 400° C. All variables are non-dimensionalized by a characteristic velocity, length scale and wall temperature.

The time integration method used to solve Eq. (2) is based on second-order semi-implicit fractional-step method (Kim & Moin, 1985, Le & Moin, 1991). For convection terms in Eqs. (3) and (4), we use the second-order Crank-Nicolson method for the streamwise direction and a third-order Runge-Kutta method for the spanwise and wall-normal directions. Also, we use time lagging method for $\mu(C)$ and explicit Euler method for $S(T,C)$. All the spatial derivatives in Eq. (2) are resolved with the second-order central-difference scheme and the hybrid scheme (QUICK and second-order central-difference scheme) is used in Eqs. (3) and (4).

2.3 Computational details

The computations were carried out for a Reynolds number of 5600 based on the bulk velocity u_b and the channel half-width δ. The Schmidt number is difficult to define because its variation in the fouling process so we assumed the Schmidt number of 5. The Prandtl number of 2.88 were used for the computation (Bennett *et al.*, 2011).The streamwise and spanwise computational domains are 12 δ

and 3δ, respectively. The grid points used are $256 \times 129 \times 128$ in the x, y and z directions, respectively.

The fully developed channel flow was calculated for a same domain and the results from the calculation were used for the inlet boundary condition. Convective boundary condition were used for the outlet of the channel. The Neumann boundary condition was used to calculate the volume fraction at the wall. For investigating fouling accumulation in the lower all, the constant non-dimensionalized temperatures at the upper wall and lower wall set to -1 and 1, respectively. Also, we used periodic boundary condition in the spanwise direction. FIGURE 2.3 shows boundary conditions of the present study.

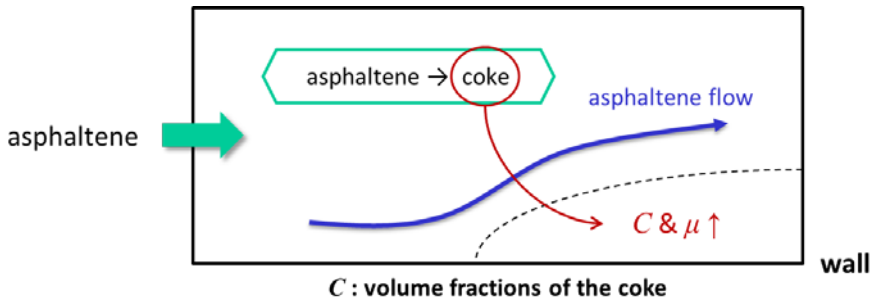

FIGURE 2.1 The schematic diagram of the process of fouling deposition

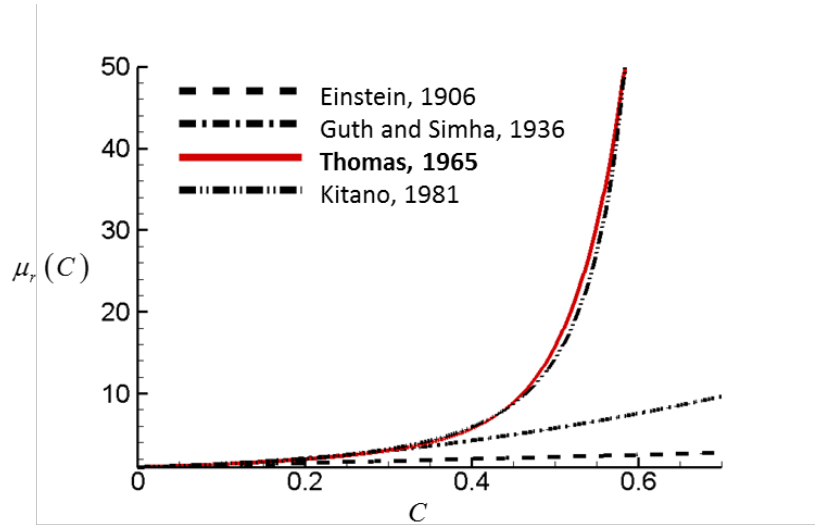

FIGURE 2.2 Volume fraction of solid versus relative viscosity with different equations.

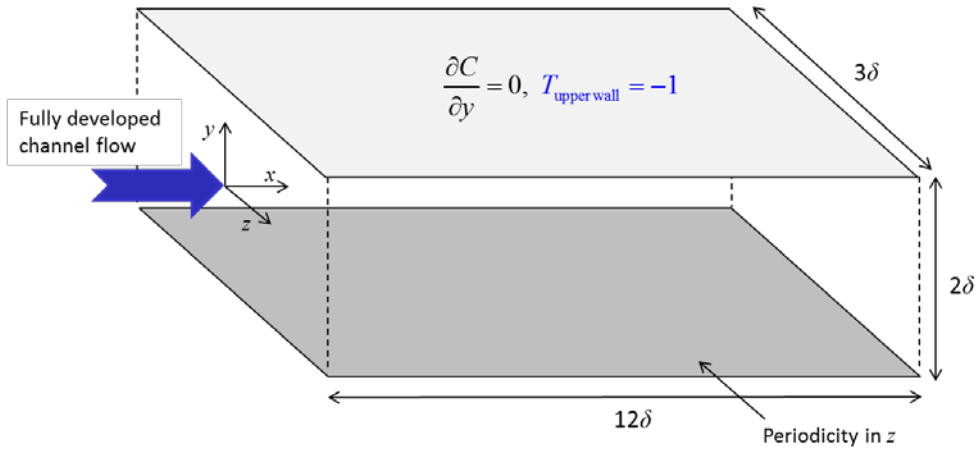

FIGURE 2.3 The boundary conditions of the present study

Chapter 3

Results and discussion

3.1 Mean streamwise velocity and mean temperature of the fouled channel

We have performed direct numerical simulation of three-dimensional channel flow with fouling accumulation. Contours of mean streamwise velocity and mean temperature at non-dimensionalized time of 300 is shown in FIGURE 3.1. The instantaneous streamwise velocity and temperature is averaged in spanwise direction. Details are below.

$$\bar{u} = \frac{1}{L_z}\int u dz, \quad \bar{T} = \frac{1}{L_z}\int T dz.$$

The streamwise velocity decreases near the lower wall along the streamwise direction. As the streamwise velocity decreases near the lower wall, the temperature of the lower wall also decreases due to weak convection.

FIGURE 3.2 shows the mean streamwise velocity profiles at x/δ = 2, 6 and 10, respectively. The streamwise velocity near the lower all decreases because coke deposits at the wall by its high viscosity. After all, the mean velocity of the channel increases along the streamwise direction

3.2 Growth of the fouling boundary along with the high viscosity at the wall

Contours of the instantaneous volume fraction of coke (C) and viscosity (μ_r) is shown in FIGURE 3.3. As time passed, the volume fraction of coke increases near the lower wall by reaction. And as the volume fraction of coke increases, the viscosity near the lower wall also increses.

Contours of the instantaneous spanwise vorticity as time increases is shown in FIGURE 3.4. As time passed, the vortices are weakend near the wall and the shear layer moves upward due to the low velocity in the deposition.

FIGURE 3.5 shows contours of the dimmed instantaneous spanwise vorticity and the iso-line that the non-dimensionalized streamwise velocity equals 0.01 as time increases. The near wall vortical structures travel over the iso-line and the shear layer appears above the line. Thus, we can assume that this line is a boundary of fouling. The contours of the instantaneous streamwise vorticity and iso-line that the non-dimensionalized streamwise velocity equals 0.01 at $tu_b / \delta = 300$ is shown in FIGURE 3.6. The cross wise planes are chosen at x/δ=2, 6 and 10. As the volume fraction of coke increases along the streamwise direction, vortices vanish under the interface due to high viscosity. Also, the wavy shape of fouling surface is developed due to the strong vortices near the boundary.

3.3 Changes of the fouling boundary due to near wall vortical structures

Contours of vortical structures and the boundary of fouling is shown in FIGURE 3.7. Vortical structures vanish at downstream of the channel due to high viscosity. FIGURE 3.8 shows contours of streamwise vorticity and iso-line that the non-dimensionalized streamwise velocity equals 0.01 at x/δ=10. As time passed the vortices travel over the boundary of fouling and the shape of boundary changes due to near wall vorticies. FIGURE 3.9 shows instantaneous velocity vectors and iso-line of u/u_b=0.01, 0.05 and 0.1 at x/δ=10. The blue arrow means strong vortex near the boundary of fouling. The boundary of fouling changes due to the induced flow by vortices near the peak of the fouling surface. After all, the surface of fouling has more wavy shape than before.

3.4 Time traces of fouling resistance and the boundary of fouling

Fouling resistance is a significant value to determine how much accumulation occurred. The definition of fouling resistance is below,

$$R_f(x,t) = \left(\frac{T_w - T_b}{q}\right)_{x,t} - \left(\frac{T_w - T_b}{q}\right)_{x,0},$$

where T_w and T_b mean wall and bulk temperatures and q means heat flux. Also, k means thermal conductivity. FIGURE 3.10 shows fouling curves (Bohnet, 1987). m_d means deposition rate and m_r means removal rate of fouling. There are three phases of fouling which are induction, transition and fouling. Also, there are three essentially

different cases. Case 1 shows constant increase of fouling resistance and case 2 shows slowing down of deposition process and case 3 shows converging fouling resistance. The causes of differences between cases are that which process is dominant in time. Also, Bohnet said phases 1 and/or 2 need not necessarily occur.

FIGURE 3.11 shows fouling curves from Bennett *et al.*(2011) and the present study. Bennett *et al.* conducted experiments of crude oil fouling in a hot pipe. Fouling resistance obtained from Bennett *et al.* has no induction and transition periods which is similar to the result of the present study. The fouling curves does not attain a maximum. In earlier time region, the deposition process of fouling process is dominant and after that, the removal process of fouling process is dominant. FIGURE 3.12 shows contours of fouling boundary colored with non-dimensionalized wall-normal location in the fouling phase. In this phase of the present study, the deposition and removal processes is retained in time but the deposition is slowing down with increasing thickness of layer. Yellow part means lower location and red, black means higher location. The boundary of fouling moves up and down during accumulation.

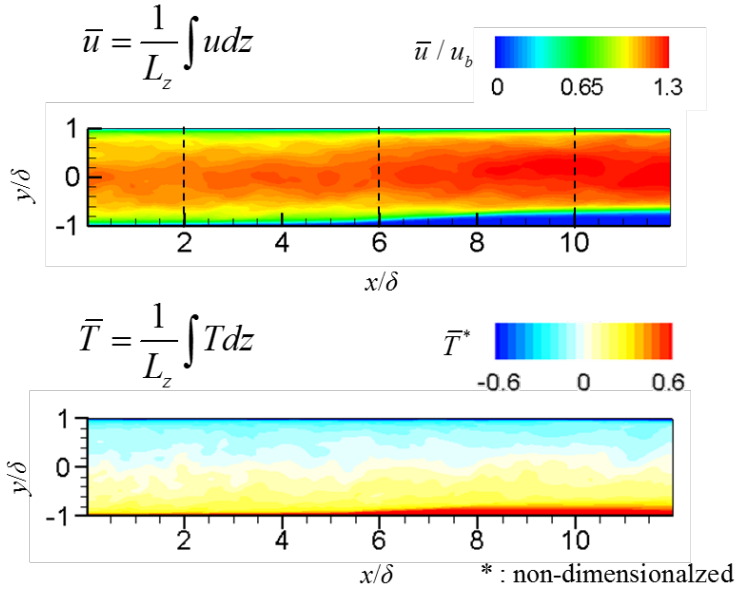

FIGURE 3.1 Contours of mean streamwise velocity and mean temperature at non-dimensionalized time of 300

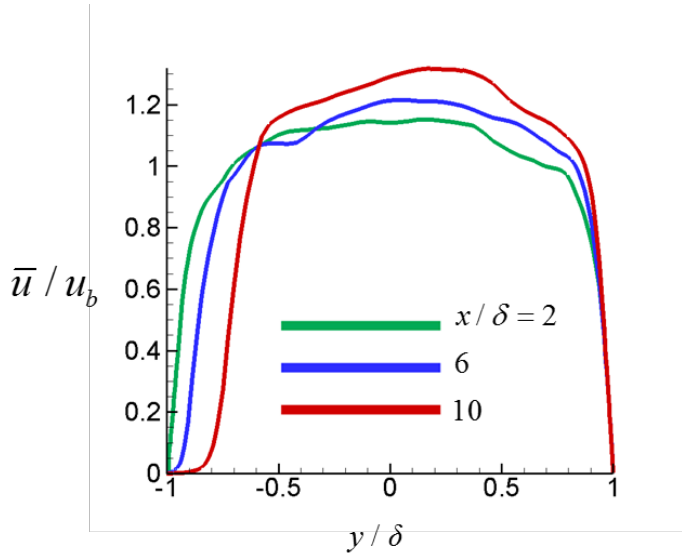

FIGURE 3.2 shows the mean streamwise velocity profiles at x/δ = 2, 6 and 10, respectively.

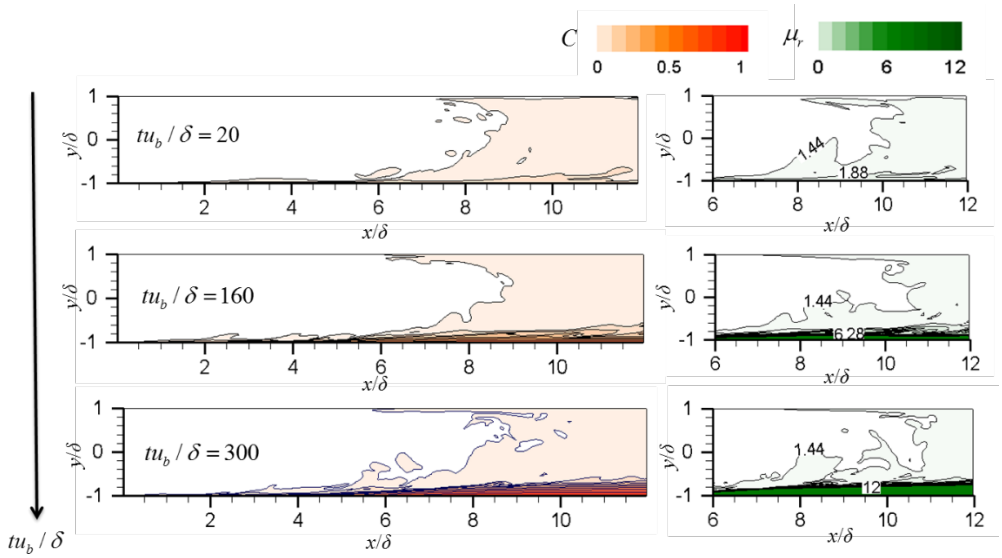

FIGURE 3.3 Contours of instantaneous volume fraction of coke and viscosity.

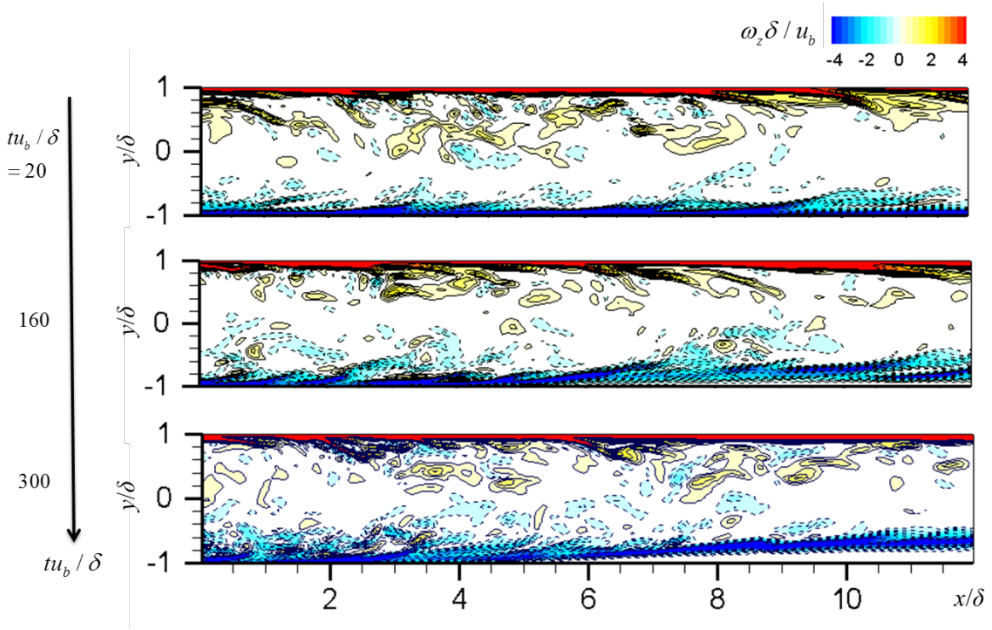

FIGURE 3.4 Contours of the instantaneous spanwise vorticity

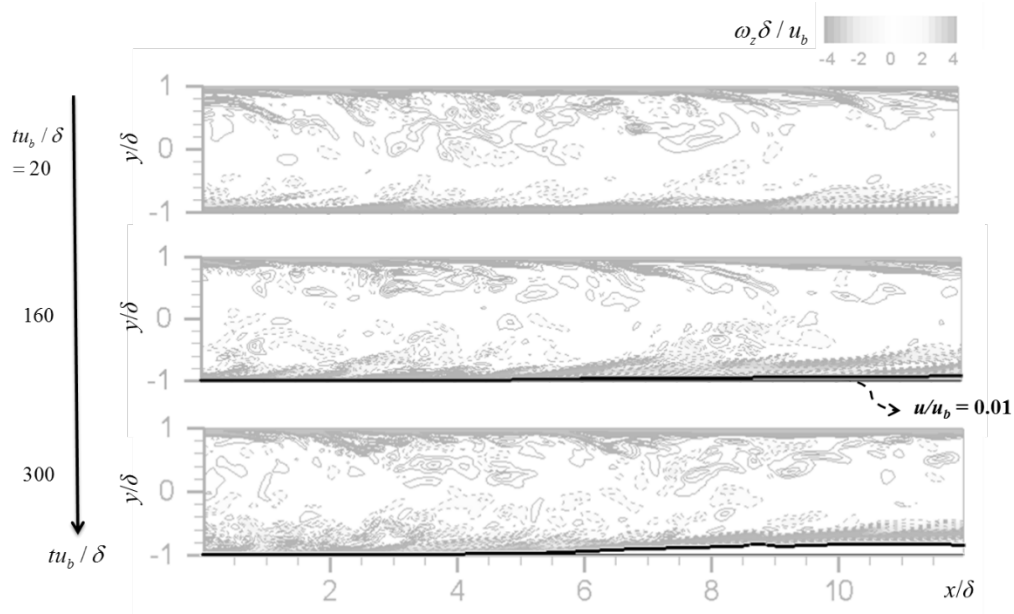

FIGURE 3.5 Contours of the instantaneous spanwise vorticity and the iso-line that the non-dimensionalized streamwise velocity equals 0.01

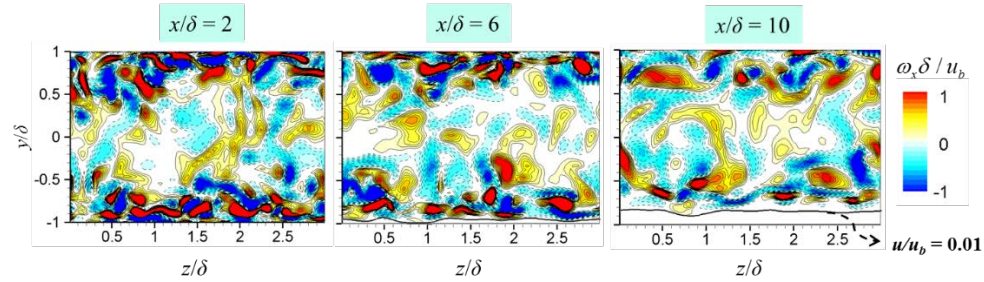

FIGURE 3.6 Contours of instantaneous streamwise vorticity and the iso-line that the non-dimensionalized streamwise velocity equals 0.01 at tu_b/δ=300

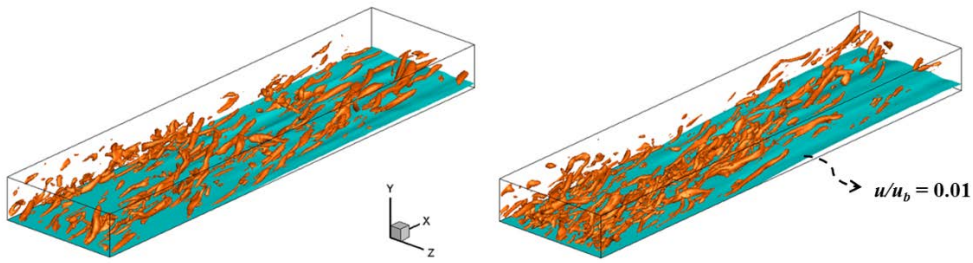

FIGURE 3.7 Contours of vortical structures based on λ_2=−0.4 and the iso−line that the non−dimensionalized streamwise velocity equals 0.01.

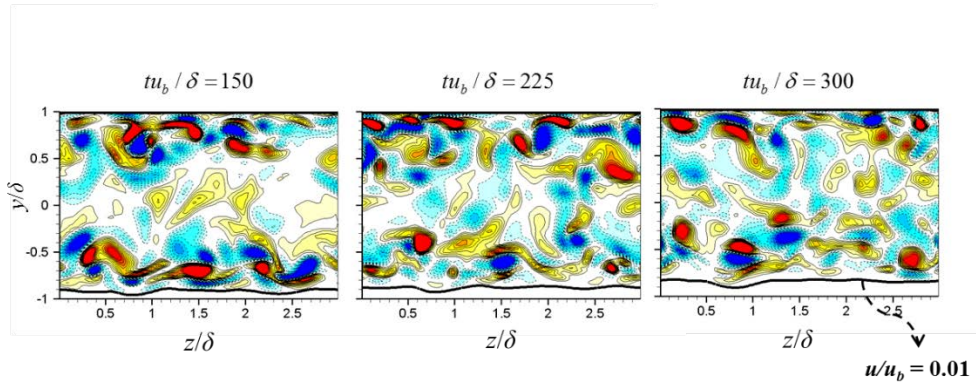

FIGURE 3.8 Contours of streamwise vorticity at x/δ=10 and the iso-line that the non-dimensionalized streamwise velocity equals 0.01 with different times

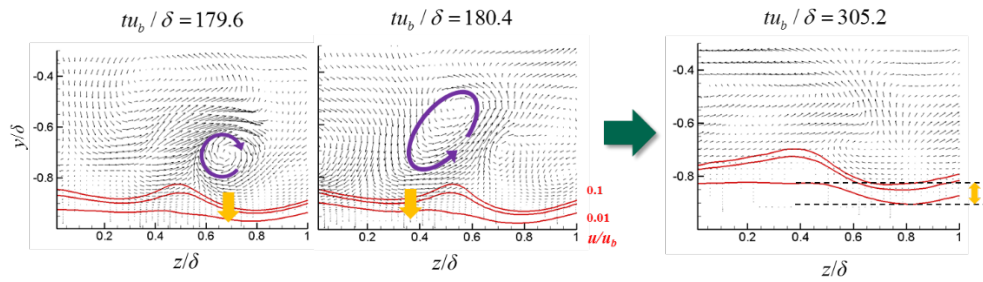

FIGURE 3.9 Instantaneous velocity vectors and iso-line that the non-dimensionalized streamwise velocity equals 0.01, 0.05 and 0.1 with different times.

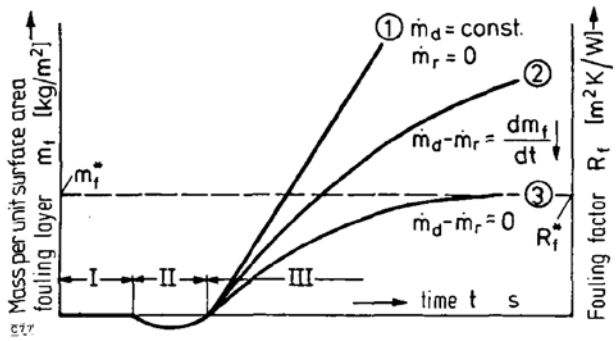

FIGURE 3.10 Fouling curves : Ⅰ. induction, Ⅱ. transition, Ⅲ. fouling (Bohnet, 1987)

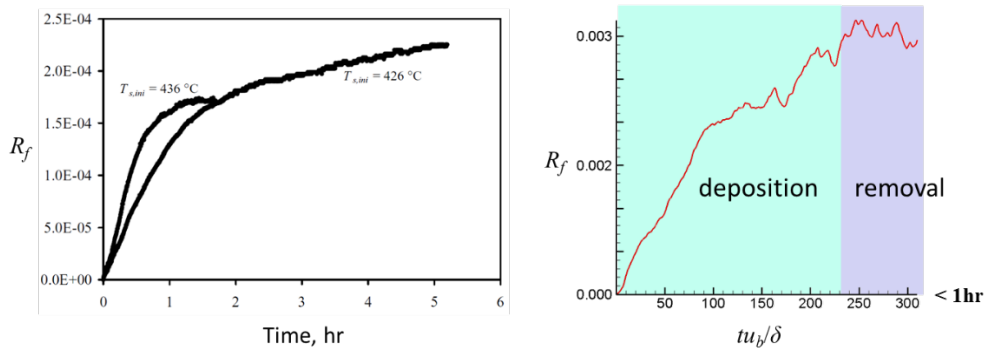

FIGURE 3.11 Fouling curves from Bennett et al., 2011 (left) and the present study (right)

Chapter 4

Summary and conclusion

In the present study, we conducted direct numerical simulation of a turbulent channel flow with a chemical reaction fouling by assuming coke as a highly viscous fluid.

We simulated the growth of fouling near the wall using equations of the relative viscosity and the reaction rate models.

As coke deposits, the relative viscosity became higher and the vortices were weakened.

The streamwise elongated surface of fouling is developed by the near wall streamwise vortices.

We will conduct simulations at higher Reynolds number and will verify results of the simulation with experimental data of chemical reaction fouling.

Bibliography

Müller-Steinhagen, H., M. R. Malayeri, and A. P. Watkinson. "Fouling of heat exchangers-new approaches to solve an old problem." Heat transfer engineering 26.1 (2005): 1-4.

Zhi-Ming, Xu, Z. H. A. N. G. Zhong-Bin, and Y. A. N. G. Shan-Rang. "Costs due to utility fouling in china." (2007): 113.

Helalizadeh, Abbas, H. Müller-Steinhagen, and M. Jamialahmadi. "Mixed salt crystallisation fouling." Chemical Engineering and Processing: Process Intensification 39.1 (2000): 29-43.

Mwaba, M. G., et al. "Experimental investigation of CaSO4 crystallization on a flat plate." Heat transfer engineering 27.3 (2006): 42-54.

Macchietto, S., et al. "Fouling in crude oil preheat trains: a systematic solution to an old problem." Heat Transfer Engineering 32.3-4 (2011): 197-215.

Brahim, Fahmi, Wolfgang Augustin, and Matthias Bohnet. "Numerical simulation of the fouling process." International Journal of Thermal Sciences 42.3 (2003): 323-334.

Sileri, D., et al. "Mathematical modelling of asphaltenes deposition and removal in crude distillation units." International Conference on Heat Exchanger Fouling and Cleaning VIII. Vol. 2009. Austria: Schladming, 2009.

Bayat, Mahmoud, et al. "CFD modeling of fouling in crude oil pre-heaters." Energy Conversion and Management 64 (2012): 344-350.

Einstein, Albert. "Eine neue bestimmung der moleküldimensionen." Annalen der Physik 324.2 (1906): 289-306.

Guth, Eugene, and R. Simha. "Untersuchungen über die viskosität von

suspensionen und lösungen. 3. über die viskosität von kugelsuspensionen." Colloid & Polymer Science 74.3 (1936): 266-275.

Thomas, David G. "Transport characteristics of suspension: VIII. A note on the viscosity of Newtonian suspensions of uniform spherical particles." Journal of Colloid Science 20.3 (1965): 267-277.

Kitano, T., T. Kataoka, and T. Shirota. "An empirical equation of the relative viscosity of polymer melts filled with various inorganic fillers." Rheologica Acta 20.2 (1981): 207-209.

Akmaz, S., Deniz, C. U. and Yasar, M. "Investigation of Reaction Pathways and Kinetics of Turkish Asphaltenes," Chemical Engineering Transactions 32 (2013): 871~876.

Kim, John, and Parviz Moin. "Application of a fractional-step method to incompressible Navier-Stokes equations." Journal of computational physics 59.2 (1985): 308-323.

Le, Hung, and Parviz Moin. "An improvement of fractional step methods for the incompressible Navier-Stokes equations." Journal of Computational Physics 92.2 (1991): 369-379.

난류 평판 유동에서 화학반응 파울링에 대한 직접수치모사

서울대학교 대학원
기계항공공학부
김한별

요약

본 연구에서는 Re = 5600일 때에 난류 평판유동에서 화학반응 파울링에 대한 직접수치해석을 수행하였다. asphaltene과 coke 사이의 단일반응을 가정하였으며, coke를 높은 점성을 가지는 유체로 가정하였다. 스칼라 운송 방정식을 통해 평판 내부의 온도와 coke의 부피율을 계산하였으며, 상대 점성계수와 반응 속도 항의 경우 coke의 특성을 묘사할 수 있도록 모델링하였다.

그 결과, 높은 온도의 벽에 파울링 층이 형성되었으며 시간에 따라 점진적으로 파울링 층이 두터워짐을 확인하였다. 파울링 층이 두터워짐에 따라 침적속도는 감소한 반면, 탈락 속도는 증가하여 경계층의 상승 속도는 점차 감소함을 보였다. coke가 침적됨에 따라 높은 점성으로 인해 평판 하류로 갈수록 와류가 감소하였으며, 경계층 주변 와류로 인해 난류구조가 유동방향으로 가늘고 긴 형상을 가짐을 보였다.

주요어 : CFD, 모델링, 화학반응 파울링, 아스팔틴, 평판 유동

학번 : 2012-23939